Analyst

ROYAL SOCIETY OF CHEMISTRY

PAPER

View Article Online
View Journal | View Issue

Cite this: *Analyst*, 2021, **146**, 4545

Electrochemical flow injection analysis of the interaction between pyrroloquinoline quinone (PQQ) and α-synuclein peptides related to Parkinson's disease†

Shaopei Li, Meissam Noroozifar, Jiayun Zhou and Kagan Kerman *

α-Synuclein (α-syn) is a hallmark protein of Parkinson's disease (PD). The aggregation process of α-syn has been heavily associated with the pathogenesis of PD. With the exponentially growing number of potential therapeutic compounds that can inhibit the aggregation of α-syn, there is now a significant demand for a high-throughput analysis system. Herein, a novel flow injection analysis system with an electrochemical biosensor as the detector was developed to study the interaction of a well-described antioxidant and amyloid inhibitor, pyrroloquinoline quinone (PQQ) with α-synuclein peptides. Screen-printed gold electrodes (SPEs) were modified using heptapeptides from α-syn wild-type (WT) and mutants such as lysine knock-out (ETEE) and E46K. Affinity binding events between these peptides and PQQ were analyzed by electrochemical impedance spectroscopy (EIS) and further confirmed by high-performance liquid chromatography (HPLC), liquid chromatography/mass spectrometry (LC/MS), and nuclear magnetic resonance (NMR) spectroscopy. HPLC and LC/MS results revealed that PQQ formed a stable complex with α-syn. NMR results confirmed that the α-syn–PQQ complex was formed *via* a Schiff base formation-like process. In addition, results showed that lysine residues influenced the binding event, in which the presence of an extra lysine stabilized the α-syn–PQQ complex, and the absence of a lysine significantly decreased the interaction of α-syn with PQQ. Therefore, we concluded that EIS is a promising technique for the evaluation of the interaction between PQQ-based amyloid inhibitors and α-syn. The electrochemical flow injection analysis assembly provided a rapid and low-cost drug discovery platform for the evaluation of small molecule–protein interactions.

Received 22nd April 2021,
Accepted 26th May 2021

DOI: 10.1039/d1an00698c

rsc.li/analyst

Introduction

The prevalence of Parkinson's disease (PD), a neurodegenerative disorder that targets human motor functions, is on the rise. To the best of our knowledge, no cure has been reported for PD. A hallmark protein, α-synuclein (α-syn), has been implicated in the development of PD and is 140-aa long, containing seven groups of mutant repeats of KTKEGV.[1] The protein is subdivided into three major regions: an amphipathic N-terminal region, a non-amyloid component (NAC), and an acidic C-terminal region.[2,3] In a monomeric form, α-syn can exist as a free-flowing random coil or it can bind to the lipid membrane forming an α-helical structure. Once triggered, both forms of monomeric α-syn can aggregate into oligomers, then into β-sheet-rich fibrils, and eventually into Lewy body inclusions.[4] This progression of α-syn secondary structures has been linked to PD progression.[5] With each stage of proteomic rearrangement, several factors can increase the overall aggregation process. The presence of reactive oxygen species (ROS) facilitates the increase of oligomer aggregation, accelerates the aggregation of truncated α-syn mutants, and thus increases the oligomer cellular toxicity.[6,7] In addition, the presence of biometals, such as copper, can also increase the overall aggregation rate by facilitating a long-range contact between residues 41–47 and 52–67 at the NAC of α-syn resulting in a more rapid intra- and intermolecular rearrangement.[8] The presence of biometal ions can also fuel the production of ROS, causing neurotoxicity and accelerating the α-syn aggregation process.[9] Therefore, recent studies have indicated that the suppression of the aggregation of α-syn at an early stage could be highly beneficial.[8,9]

Several small molecules have been shown to modulate α-syn aggregation.[10,11] Among the diverse groups of naturally occurring small molecules, pyrroloquinoline quinone (PQQ)

Department of Physical and Environmental Sciences, University of Toronto Scarborough, 1265 Military Trail, Toronto, ON, M1C 1A4, Canada.
E-mail: kagan.kerman@utoronto.ca

†Electronic supplementary information (ESI) available. See DOI: 10.1039/d1an00698c

has been attracting attention from researchers. PQQ exhibits antioxidative effects that have been shown to facilitate cellular growth.[12,13] In a previously published work, it was found that the presence of PQQ prevented the fibrillation of α-syn, and it was hypothesized that PQQ was able to achieve this by forming a Schiff base formation with the lysine residues within α-syn.[14] To the best of our knowledge, no direct evidence has been presented to support this hypothesis. Therefore, it has been of great interest to understand how PQQ interacted with α-syn to suppress fibrillogenesis. To investigate this, a biosensing platform was developed in this study as a useful tool to monitor the PQQ–α-syn interactions. The use of fragmentation of peptides to study the binding behaviors between α-syn and potential therapeutic small molecules is a feasible approach; as α-syn naturally retains a random coil structure, major conformational changes only occur during or after aggregation.[15] Recently, the use of peptide fragments to understand certain characteristics of a protein has been proven to be successful.[16] Using peptide fragments allowed obtaining residue-specific information which arguably is more critical in amyloid-forming proteins. The residues 41–47 are particularly of major interest since the Cu(II) ion binding site of His-50 is located in proximity to this repeat unit.[17] The aggregation enhancing point mutation E46K also occurs in this region.[18] Furthermore, since PQQ has been hypothesized to interact with the lysine residues, this fragment of the protein was selected as the first model peptide fragment in this study.

Flow injection analysis has been adopted into a variety of analytical studies.[19–22] Flow cells simplify and streamline the analysis of low volumes of samples, which is extremely critical when evaluating novel small drug molecules that are available only in small quantities.[23] Several leading studies have demonstrated the feasibility of electrochemical systems in studying the aggregation of α-synuclein and its interactions with biomolecules.[24–27] Therefore, it has become clear that combining the flow injection analysis with an electrochemical biosensor can yield a new generation of powerful analytical platforms for the pre-screening of potential therapeutic molecules for PD. In this proof-of-concept study, we have constructed a novel platform that allowed the evaluation of PQQ binding affinity towards α-syn peptide fragments. Residues 41–47 were first attached at the N-terminus using 3-mercaptopropanoic acid (3-MPA) to allow for surface immobilization on a screen-printed gold electrode (SPE). Using automated syringe pumps connected to a homemade four-way mixing valve, a flow cell designed specifically for SPEs was incorporated to complete the flow injection analysis system. Cyclic voltammetry (CV) and electrochemical impedance spectroscopy (EIS) were performed to monitor the electrode surface modification steps. EIS was also used to analyze the complexation formed between PQQ and α-syn peptides. In parallel with electrochemical studies, sophisticated analytical techniques such as high-performance liquid chromatography (HPLC), liquid chromatography/mass spectrometry (LC/MS), and nuclear magnetic resonance (NMR) spectroscopy were applied to confirm the complex formation between PQQ and α-syn peptides.

Materials and methods

Pyrroloquinoline quinone (95%, PQQ) was purchased from Sigma-Aldrich (Oakville, ON) and was used as received. The non-modified heptapeptides, as well as the heptapeptides modified with 3-mercaptopropanoic acid (3-MPA) at the N-terminus (Table 1), were purchased from CanPeptide (Montréal, QC).

All electrochemical experiments were carried out using an Autolab PGSTAT 128 N (Metrohm, Utrecht, the Netherlands) potentiostat/galvanostat controlled by the NOVA 2.1 software (Metrohm, Utrecht, the Netherlands). EIS was conducted over a frequency range of 0.1 Hz to 100 kHz with 0.02 V amplitude (rms) in 10 mM $[Fe(CN)_6]^{3-/4-}$ with 0.1 M $NaClO_4$. Non-modified heptapeptides were dissolved in 10 mM PBS and combined with a desired concentration of PQQ. The mixture was incubated overnight with gentle shaking. HPLC analyses were performed with an Agilent Technology 1260 Infinity (Santa Clara, CA) system, equipped with a diode array UV-vis detector and a Vydac C18 column (4.6 × 250 mm, 5 μM df). The solvents used were acetonitrile (HPLC grade, VWR, Radnor PA) as solution-A and ultrapure water (18.2 MΩ Milli-Q water, Millipore Canada) as solution-B, both containing 0.1% TFA (Sigma-Aldrich, Oakville ON) with a flow rate of 0.500 mL min^{-1} with solution-A from 5% to 65% in 20 min. The mass spectra were obtained using an Agilent 6500 LC/MS electrospray ionization mass spectrometer (ESI-MS, Santa Clara, CA) fitted with an Agilent Poroshell 120-C18 column (3.0 × 100 mm, 2,7 5 μM df).

Screen-printed gold electrodes (DS220AT, SPEs) that were purchased from Metrohm DropSens (Metrohm Canada, Mississauga, ON), consisted of a working gold electrode of 4 mm diameter, a gold counter electrode, and a reference AgCl electrode. Before use, the electrodes were rinsed with ultrapure water and ethanol (97% (v/v), Sigma-Aldrich, Oakville, ON) to remove any surface-adsorbed contaminants. From the stock solution of 3-MPA-modified heptapeptides, an aliquot (10 μL) of peptides was used to prepare fresh solutions in 10 mM phosphate buffer solution (pH 7.4) and drop-cast onto the working electrode surface for overnight incubation at 4 °C. The peptide-modified electrodes were rinsed thoroughly with 10 mM PBS (pH 7.4) before use.

Electrochemical flow injection analysis

An illustrative diagram of the flow injection analysis system with a homemade four-way valve system is shown in Scheme 1. A Kd Scientific KDS210 Inf/Wid syringe pump (KD Scientific,

Table 1 Molecular information of the lysine-rich region 41–47 of WT and mutant α-syn peptides

Peptide code	Peptide sequence	Molecular weight ($g\ mol^{-1}$)
ETEE	GSETEEG	707.64
	3-MPA-GSETEEG	795.76
WT	GSKTKEG	705.75
	3-MPA-GSKTKEG	793.88
E46K	GSKTKKG	704.82
	3-MPA-GSKTKKG	792.95

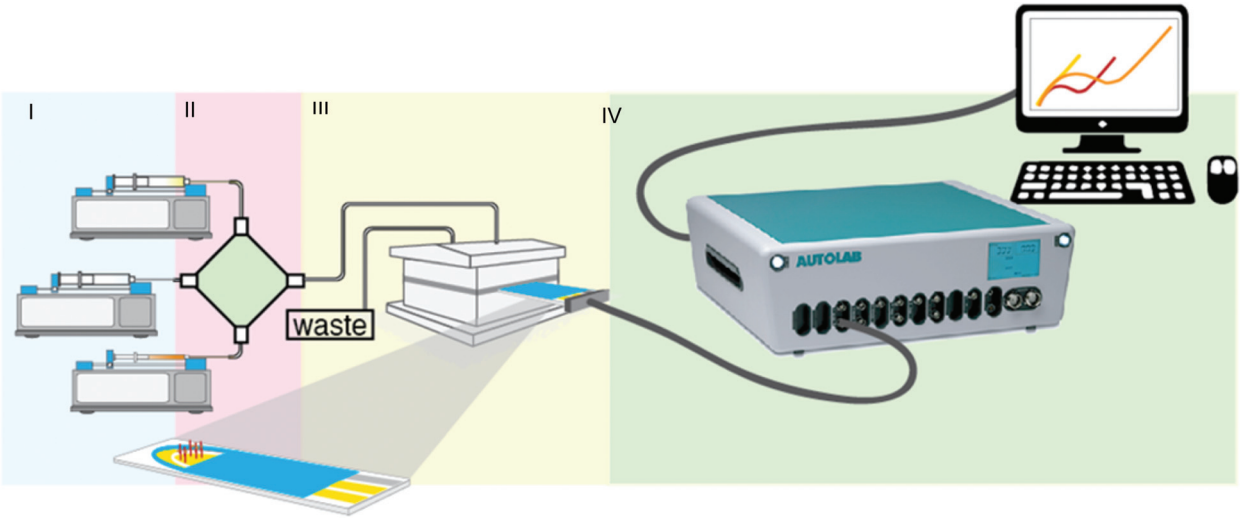

Scheme 1 Schematic illustration of the electrochemical flow injection analysis system. Section-I shows the syringes attached to the pump. Section-II represents the homemade four-way valve system connecting the syringes with the flow cell. Section-III shows the electrochemical flow cell with the SPE-based biosensor inserted into the cell with section-IV linking the flow cell to the potentiostat for electrochemical measurements.

Holliston, MA) was used to pump carrier-streams through the manifold at a flow rate of 1 mL min^{-1} for 10 mM PBS and 10 mM $[Fe(CN)_6]^{3-/4-}$ containing 0.1 M $NaClO_4$ as the supporting electrolyte and a desired concentration of PQQ at a flow rate of 0.02 mL min^{-1}. Manifold lines consisted of 1-mm i.d. polyethylene tubing. BD 309661 syringes (Becton Dickinson, Franklin Lakes, NJ) were used for delivering 10 mM $[Fe(CN)_6]^{3-/4-}$ as the redox probe. The third syringe was a 1-mL Hamilton 80700 glass syringe (Hamilton, Franklin, MA) that contained various concentrations of PQQ. The fourth inlet was connected to the DropSens flow cell (FLWCL, Metrohm Canada, Mississauga, ON) for SPEs.

NMR spectroscopy analyses and sample preparation

For the NMR analysis, the heptapeptides and PQQ solutions were prepared by dissolving the analytes in ultrapure water to create a stock concentration of 4 mM. Then, the stock solutions were further diluted with 90% ultrapure water and 10% D_2O (Millipore-Sigma, Mississauga, ON) solution to reach the final concentration of 2 mM. The heptapeptide–PQQ mixtures were mixed well and sealed and then left for slow shaking at room temperature for 24 h. Then, 20 μL of D_2O was added into the mixture resulting in the final 90% ultrapure water and 10% D_2O mixture. The water suppression ^1H proton (^1H-NMR) and ^1H–^1H total correlated spectroscopy (TOCSY) spectra were collected on an Agilent DD2 NMR 700 MHz spectrometer (Agilent, Santa Clara, CA).

Results and discussion

Analysis of the interaction between α-synuclein peptides and PQQ

To design a biosensor for the analysis of the interaction between α-syn peptide fragments and PQQ, the heptameric residue 41–47 region: GSKTKEG (wild-type, WT), and two other mutants GSKTKKG (E46K) and GSETEEG (Lys-knock-out, ETEE) of α-syn were studied. The 3-MPA-conjugated peptides contained thiol groups that allowed for attachment on gold surfaces. Electrochemical impedance spectroscopy (EIS) was used to monitor the peptide attachment process on SPEs. In addition, CV measurements were performed to monitor the redox signals of $[Fe(CN)_6]^{3-/4-}$ to confirm the immobilization of peptides on SPEs.

As shown in Fig. 1, on the bare SPEs, a semicircle correlated to the charge transfer resistance (R_{CT}) was not observed in the Nyquist plots suggesting a negligible impedance at the bare electrode surfaces. CV scans demonstrated two prominent signals at 0.175 and 0.073 V at bare SPEs corresponding to the anodic and cathodic current peaks of $[Fe(CN)_6]^{3-/4-}$, respectively. When 3-MPA-conjugated peptides were immobilized, a sharp increase of R_{CT} value to 1057.5 Ω was observed. Using 3-MPA-conjugated peptides, a significant decrease in the peak current intensity was observed with a shift in the peak potential on CV scans. This was expected, as the successful attachment of the peptides on the electrode occurred, the peptide layer slowed down the electron transfer kinetics between $[Fe(CN)_6]^{3-/4-}$ and the electrode surface resulting in the decrease of current intensity with an increase of R_{CT}. Both EIS and CV results demonstrated that the modification processes were successful, allowing the biosensor for applications in the analyses between heptapeptides and PQQ.

PQQ or methoxatin is a redox cofactor that has been shown to have antioxidant and amyloid inhibition properties, which in turn lowered its overall cellular toxicity.[28] Though PQQ has also been explored as a biomaterial with electrocatalytic properties, PQQ shows no redox activity in the potential range at which gold electrodes functioned.[29] Therefore, when PQQ interacted with the surface-immobi-

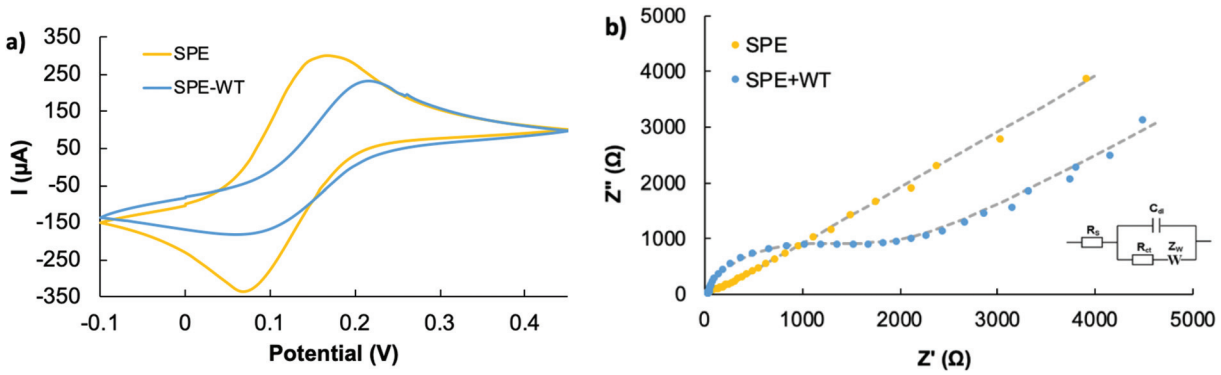

Fig. 1 (a) Cyclic voltammograms and (b) Nyquist plots of the bare SPE (yellow) and WT peptide-modified SPE (blue) with 10 mM $[Fe(CN)_6]^{3-/4-}$ as the redox probe in 0.1 M $NaClO_4$ (pH 7.0). R_{CT} values were extracted by fitting the Nyquist plots with a modified Randles equivalent circuit (as shown in the inset of (b)).

lized peptides, the attachment of PQQ resulted in the suppression of the electron transfer process between $[Fe(CN)_6]^{3-/4-}$ and the electrode surface. This led to the increase of R_{CT} and decrease in the peak currents as well as causing a shift in the peak potential of the redox probe, $[Fe(CN)_6]^{3-/4-}$ (ESI Fig. S1†). As shown in Fig. 2, after 2.5 mM of PQQ was incubated with the peptide-modified SPEs, an increase in the R_{CT} value was observed. This difference in the R_{CT} (ΔR_{CT}) was calculated as follows:

$$\Delta R_{CT} = R_{CT(\text{Peptides with PQQ})} - R_{CT(\text{Peptides alone})} - R_{CT(\text{Bare SPE})} \quad (1)$$

As a result of adopting this equation to the R_{CT} values obtained from the Nyquist plots shown in Fig. 2a–c, the ΔR_{CT} of 1441.97 ± 82.28, 3767.70 ± 77.93, and 4014.70 ± 76.94 Ω were determined for the interaction of ETEE peptides with PQQ (ETEE + PQQ), WT peptides with PQQ (WT + PQQ), and E46K peptides with PQQ (E46K + PQQ), respectively, supporting our hypothesis that the binding of PQQ with the peptides took place at the electrode surfaces. Compared to WT, ETEE demonstrated a significantly lower response to the binding of PQQ (n = 3, p < 0.0001). As suggested in the previous literature, lysine was reported to be a key residue facilitating the interaction with PQQ.[14,30] With lysine completely removed from the sequence, the peptide had negligible interactions with PQQ, resulting in a lower ΔR_{CT} observed compared to that observed with WT. In contrast, E46K displayed a higher response to PQQ compared to WT (n = 3, p < 0.01). This was attributed to the additional lysine residue present within the E46K peptide. This extra lysine residue served as an additional affinity site for PQQ resulting in a higher R_{CT} value.

To support the interaction observed between the α-syn peptides and PQQ, additional spectroscopic analyses were performed. During the sample preparation stage, it was noted that upon mixing PQQ with the peptide solution, a color change was observed. As shown in the UV-vis spectra in Fig. S2a–c,† the peptides alone did not demonstrate any significant peaks, and PQQ showed λ_{max} at 253 nm with a shoulder peak at 280 nm and a broad peak at 338 nm similar to a previous study.[15] When peptides were combined with PQQ, the ETEE + PQQ solution did not demonstrate an observable change (Fig. S2a†). For the WT + PQQ solution, a significant change in the overall UV-vis profile was observed. A bathochromic shift of the λ_{max} at 253 nm fused with the shoulder peak at 280 nm forming a new broad peak at 275 nm, and the broad peak at 338 nm also shifted to 420 nm (Fig. S2b†). A similar bathochromic shift also occurred with the E46K + PQQ interaction (Fig. S2c†). This observation was in parallel with the previously published study when the full length and truncated α-syn mutants were combined with PQQ in solution; therefore, this suggested that the α-syn peptides could also form a possible complex with PQQ.[31] This was further confirmed when HPLC and LC-MS analyses were performed to detect the formation of complexed species between α-syn peptides and PQQ.

As shown in Fig. 3a–c, a single peak was observed at 7.96 min, 6.94 min, and 7.99 min for individual peptides, ETEE, WT, and E46K, respectively. PQQ alone displayed a single peak at 11.5 min. When the peptides were incubated with PQQ, a new peak was observed in the chromatograms of WT + PQQ and E46K + PQQ at 11.32 min and 10.95 min, respectively. In contrast, for the ETEE + PQQ samples, two peaks were observed at 7.96 min and 11.5 min, which were correlated to the ETEE peptide and PQQ alone, respectively. As shown in Fig. S3,† as the concentration of PQQ increased, the newly formed peak increased at 11.32 and 10.95 min for WT + PQQ and E46K + PQQ, respectively, while the peak correlated to the free peptides decreased. These results further suggested that new complexed species were formed in the WT + PQQ and E46K + PQQ samples.

As shown in Fig. 4a–c, all the spectra showed the molecular ion peak correlated to the peptides at 708.25, 705.30, and 704.4 m/z for E46K, WT, and ETEE, respectively. All the spectra also displayed a PQQ M^+ peak as well as the sodiated PQQ M^+ peak at 330.95 and 353.3 m/z respectively. This indicated that PQQ and the peptide in the solution did not undergo degra-

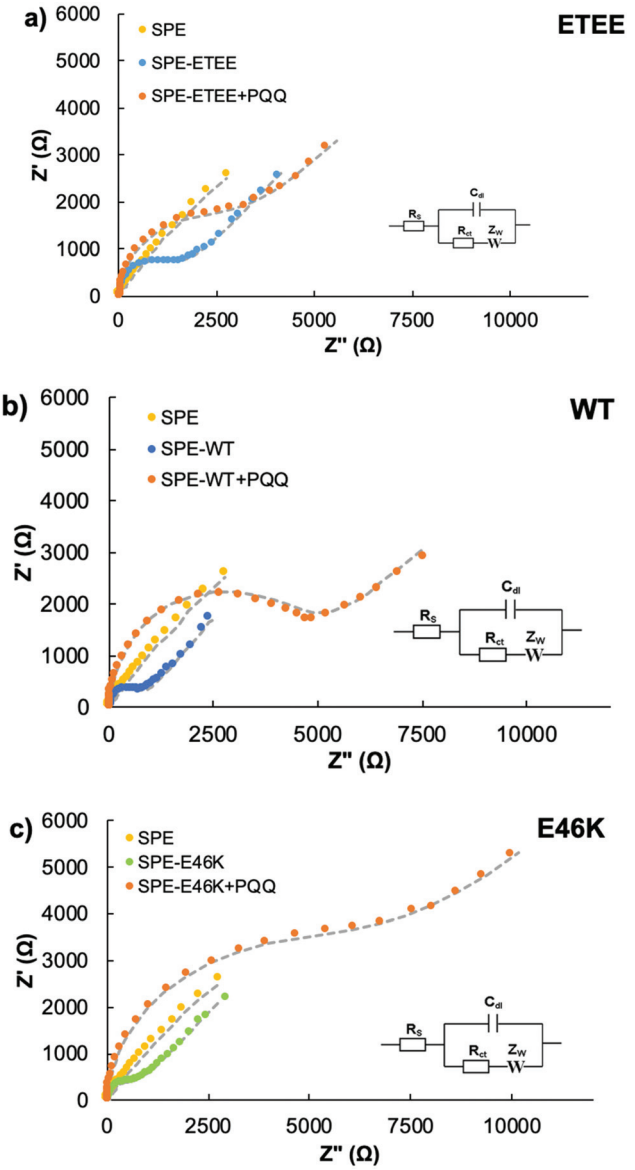

Fig. 2 Nyquist plots for the interaction between PQQ and α-syn WT and mutant peptides fitted with the modified Randles equivalent circuit (inset). The bare SPEs (yellow) were immobilized with (a, light blue) ETEE, (b, dark blue) WT, and (c, green) E46K and then incubated with 1 mM PQQ (orange). The EIS measurements were performed in 10 mM $[Fe(CN)_6]^{3-/4-}$ as the redox probe in 0.1 M $NaClO_4$ (pH 7.0).

dation during the incubation processes. In both WT + PQQ and E46K + PQQ samples, the peaks at 1016.3 and 1015.4 *m*/*z* were detected. This further suggested that the complexes of WT + PQQ and E46K + PQQ were formed.

The interaction between the heptapeptides and PQQ was further analyzed by NMR spectroscopy. As suggested in previous literature, fibrillogenesis inhibitor molecules, such as baicalein, tend to bind on the lysine residue forming a Schiff base-like structure after an initial hydrodynamic contact.[32] Furthermore, it was suggested by Kobayashi *et al.*[31] that PQQ may undergo similar binding behavior with full-length α-syn. However, one of the challenges in analyzing such interactions is the presence of hydrogen on the amine substituent of the lysine side chain that can be exchanged with solvent media, sharply decreasing its detectability. Hence, it is challenging to observe such attachment, but the protons on the hydrocarbon side chain could still provide some indication of whether PQQ has indeed attached at the predicted amine moiety. In the present study, three species of the selected heptapeptides were incubated with PQQ. Fig. 5a–c shows the down-field region of the ^{1}H-NMR 1D spectra of the heptapeptide before and after the addition of PQQ. In Fig. 5a, after the addition of PQQ, there were no observable peak shifts or a new peak generation on the ETEE + PQQ spectra. This suggested that the interaction between ETEE and PQQ did not occur as predicted. For WT peptides as shown in Fig. 5b, some major spectral differences were observed after interaction with PQQ where the 8.06 ppm triplets signal shifted up-field to 8.11 ppm, as well as new triplets and doublets were observed at 8.19 and 9.28 ppm, respectively. Similarly, as shown in Fig. 5c, the interaction of E46K peptides with PQQ resulted in a major peak shift of the triplets at 8.03 ppm to 8.08 ppm and, in addition, multiplets appeared at 8.15 ppm. The up-field regions of ^{1}H-NMR 1D spectra are shown in Fig. S4.†

To confirm the possible formation of a Schiff base between WT and E46K with PQQ, ^{1}H–^{1}H zTOCSY was performed. The up-field region of WT–PQQ spectra at the 1.4–3.2 ppm region is shown in Fig. 6a. Before exposure to PQQ, the expected $-CH_2$ lysine cluster was found at the 2.0–1.8 ppm region as well as the H_α signals (Fig. 6b). After exposure to PQQ, several changes in the spectra were observed. A decrease in the $K_{43/45}$ H_β signal intensity and a shift towards the up-field region were detected. Then, a minor decrease in the signal intensity was observed for the $K_{43/45}$ H_γ proton at 3.04 ppm. Finally, a shift towards the up-field region was also observed for both of the E_{46} H_β H_γ. This was attributed to the binding of PQQ to the lysine residue and then to the glutamate side chain forming a hydrogen bond, resulting in the shift observed on the E-46 residues, as well. For E46K species, the change observed was more pronounced. The lysine $-CH_2$ clusters and H_α were found to be shifted up-field. As shown in Fig. 6c and d, apart from the chemical shift towards the up-field region, a new signal was observed at 2.88 and 1.86 ppm with a correlation pattern similar to that of the $H_{\epsilon/\beta}$ proton observed on the hydrocarbon chain, suggesting that PQQ was bound with the lysine residue causing a major chemical shift resulting in the formation of the new signal. As suggested by our HPLC- and LC-MS-based studies, it was likely that the Schiff base was not formed to completion, but rather a carbinolamine intermediate between the peptide and PQQ occurred, which resulted in the formation of a new peak as observed in the HPLC-based studies. Also, since this intermediate was not stable and prone to fragmentation, the peptide–PQQ complex peak was not observed with high intensity in LC-MS-based results. Nevertheless, as suggested by our NMR-based

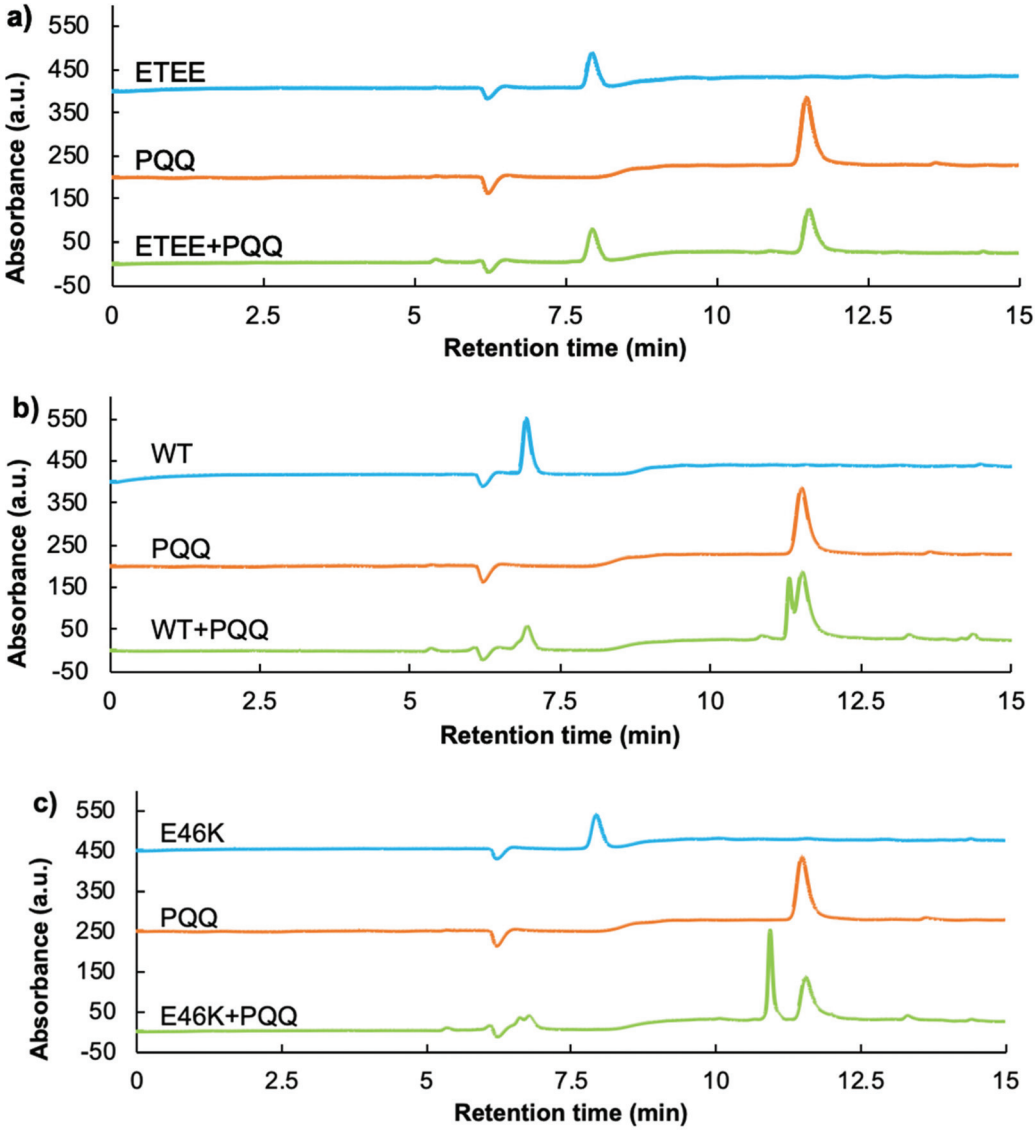

Fig. 3 HPLC chromatograms of α-syn peptides alone (blue) and PQQ alone (orange) and their equimolar mixtures (green) for (a) ETEE, (b) WT and (c) E46K peptides. The solvents used were acetonitrile (solution-A) and ultrapure water (solution-B) both containing 0.1% TFA at a flow rate of 0.500 mL min^{-1} with solution-A from 5% to 65% in 20 min with a Vydac C18 column (4.6 × 250 mm, 5 μM df).

studies, the shifts and the formation of a new signal supported our hypothesis that PQQ preferably interacted with the lysine residue of α-syn peptides. A proposed chemical structure of the PQQ–WT peptide complex is shown in Fig. S5.†

Electrochemical detection of affinity between PQQ and α-syn peptides

During the interaction with α-syn peptides (shown in Fig. 7a–c), the behaviour of PQQ resembled a Michaelis–Menten-like process with the peptide-immobilized electrode surfaces. Hence, the application of a Michaelis–Menten relationship was feasible to obtain a dissociation constant. The use of EIS to determine affinity constants was first demonstrated in the evaluation of crown ether and cations and later extended into the evaluation of the interaction between amyloid-β peptides and neurotoxins.[33–35] However, time-consuming steps were required including the incubation of an increasing concentration gradient of analytes with the modified electrodes. With the flow injection system, this issue could be easily resolved. As shown in Scheme 1, four-way valves were connected to three pumps and a flow injection chamber. SPEs were first washed by injecting blank 10 mM PBS into the flow cell at a flow rate of 1 mL min^{-1}. Background signals prior to interaction analysis were obtained at the peptide-modified electrodes by injecting an equal volume of 10 mM $[Fe(CN)_6]^{3-/4-}$ as the redox probe and EIS measurements were performed, subsequently. For the analysis of PQQ–peptide interactions, 10 mM PBS was injected, followed by PQQ solution onto the peptide-modified electrodes. An 8 min period was determined

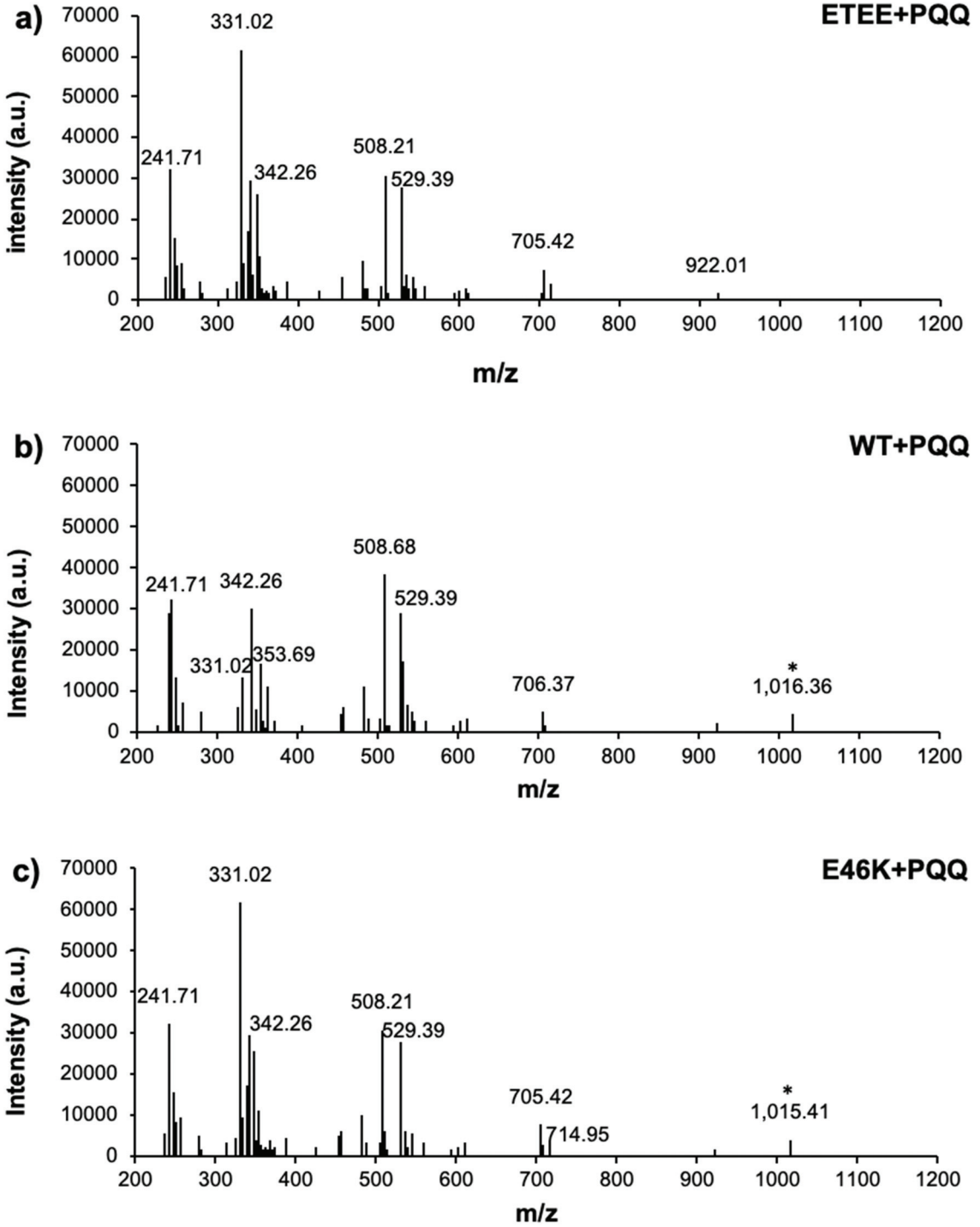

Fig. 4 LC/MS data from 500 μM α-syn peptides (a) ETEE, (b) WT and (c) E46K incubated with 500 μM PQQ overnight.

to be the optimal incubation time prior to the flow of the PBS wash solution (Fig. S6†), followed by 10 mM $[Fe(CN)_6]^{3-/4-}$ for the EIS measurements. Fig. 5a–c shows the Nyquist plots of the immobilized α-syn peptides incubated with increasing concentrations of PQQ. By fitting the Nyquist plots with the modified Randles equivalent circuit, the R_{CT} values were extracted. When the R_{CT} values were plotted against the concentration, an isotherm-like trend was observed (Fig. 5d). By applying a modified Michaelis–Menten model as shown in eqn (2), the dissociation constant was calculated:

$$\Delta R_{CT} = \frac{R_{CT(max)} \bullet [PQQ]}{K_D + [PQQ]} \quad (2)$$

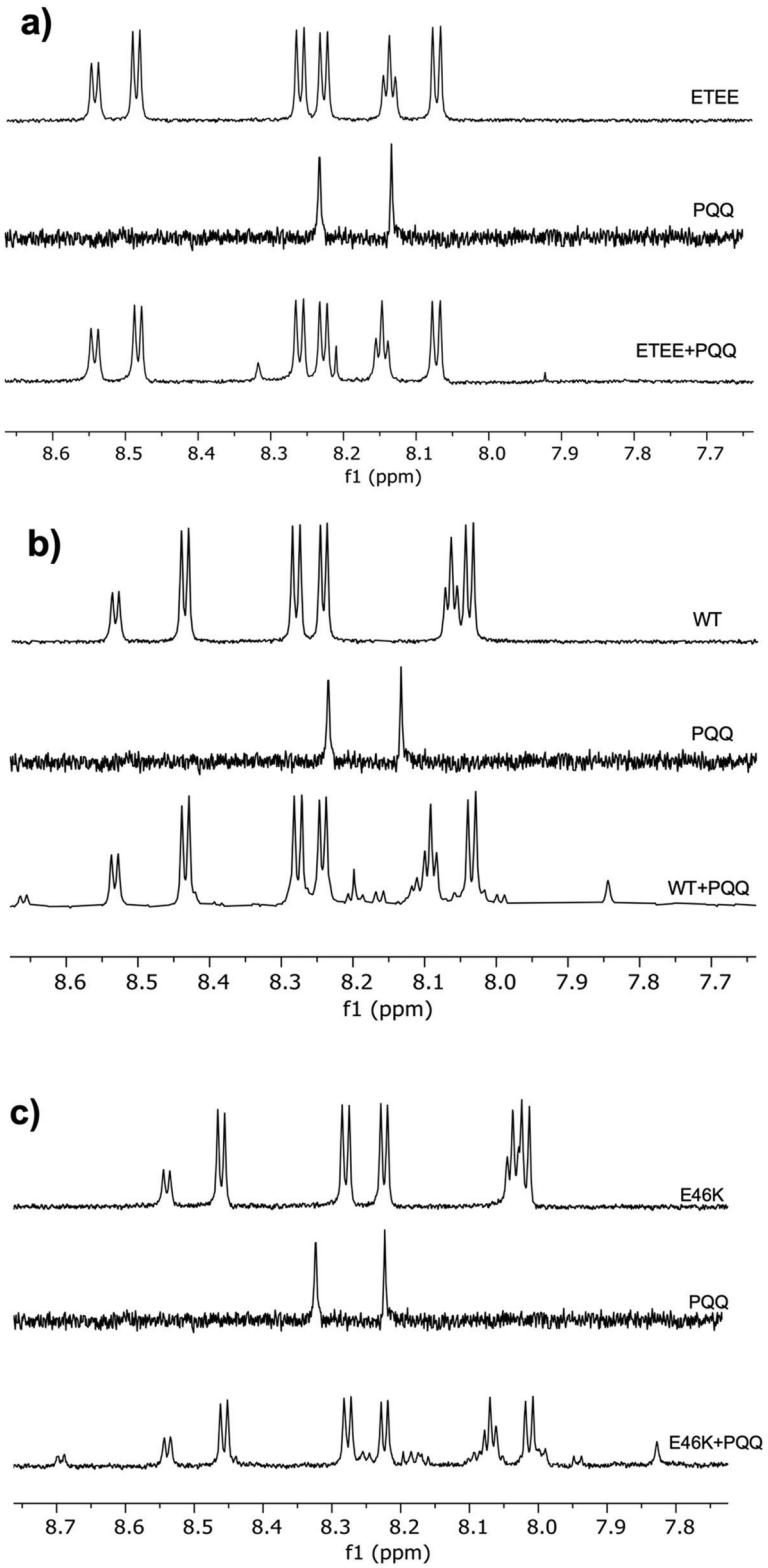

Fig. 5 ^{1}H-NMR 1D spectra of the selected region at down-field of α-syn peptides (a) ETEE, (b) WT and (c) E46K, in 90% ultrapure water with 10% D_2O at room temperature (pH 7.4).

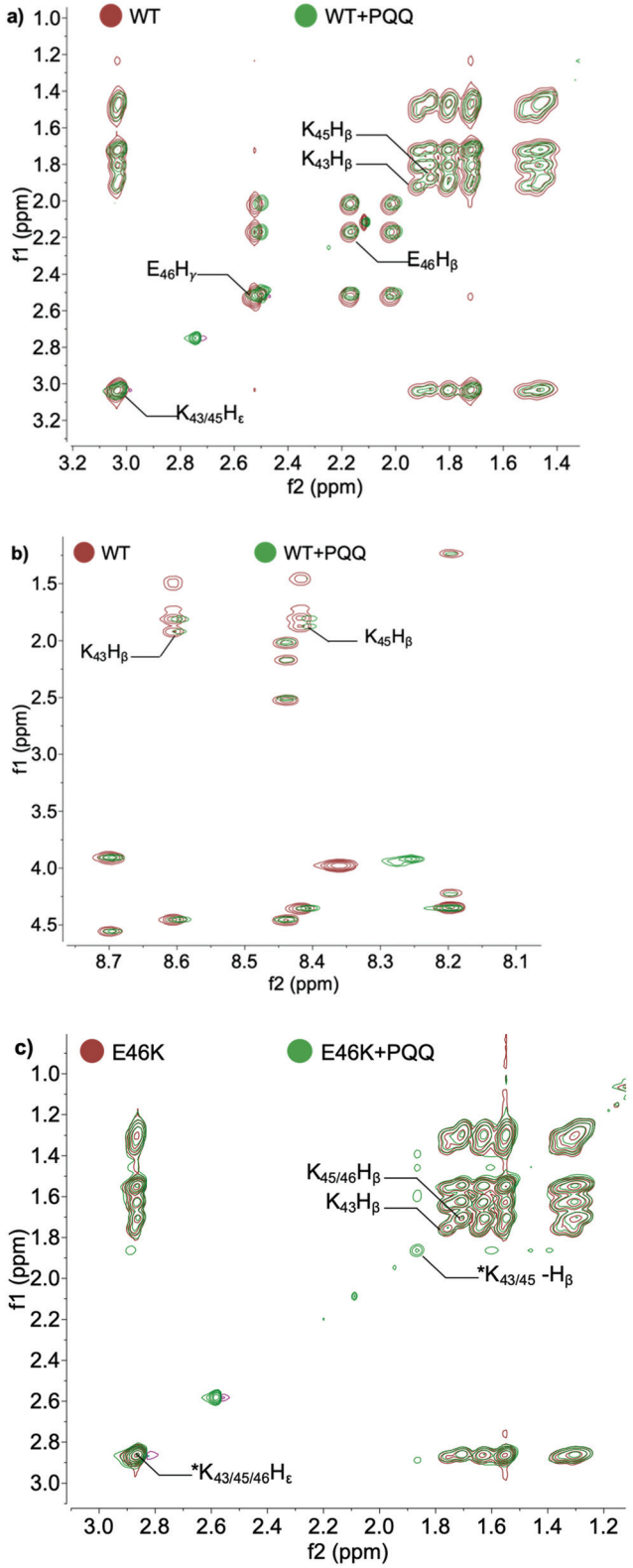

Fig. 6 2D ^{1}H–^{1}H zTOCSY spectra of the α-syn peptides collected at room temperature (pH 7.4). (a) WT split into the up-field region and (b) down-field region and E46K split into (c) the up-field region and (d) down-field region in the absence (red) and presence (green) of PQQ. (e) and (f) the structure and the proton assignment for lysine and glutamic acid residues.

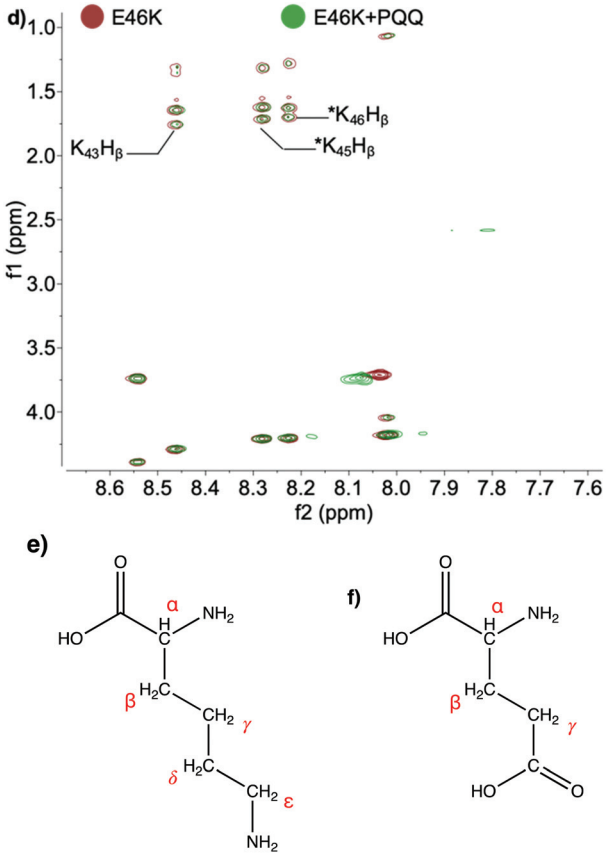

Fig. 6 *(Contd).*

where ΔR_{CT} is the change in the charge transfer resistance after incubation with PQQ, $R_{CT(max)}$ represents the charge transfer resistance of the electrode when the immobilized peptides were saturated with PQQ and [PQQ] represents the concentration of PQQ. The interaction of PQQ with ETEE demonstrated the highest K_D of 0.446 nM, followed by WT and E46K with the K_D of 0.229 and 0.143 nM, respectively. Compared to the K_D values reported by Szymańska *et al.*[33] and Grabowska *et al.*,[34] for the interaction of amyloid-β peptides with small molecules, the variation in the K_D values determined between the α-syn peptides and PQQ was of significance. Under the same experimental conditions, our EIS studies suggested that E46K had the highest affinity for PQQ. This was in parallel with the hypothesis that PQQ interacted with the lysine residues in α-syn. E46K contained one extra lysine residue, increasing the initial contact site. Furthermore, concluding from the H^1–H^1 zTOCY as well as the electrochemical results (Fig. 6a–f) that were in agreement with the literature,[14,30,36,37] we hypothesized that when PQQ interacted with the lysine residue, it was likely that the positively charged amide moiety from the neighboring extra lysine residues participated in an intramolecular stabilization process *via* electrostatic interactions between the positively charged amide and the hydroxyl-rich PQQ, decreasing the chance of detachment of PQQ from the PQQ–peptide complex. Kobayashi *et al.*[30]

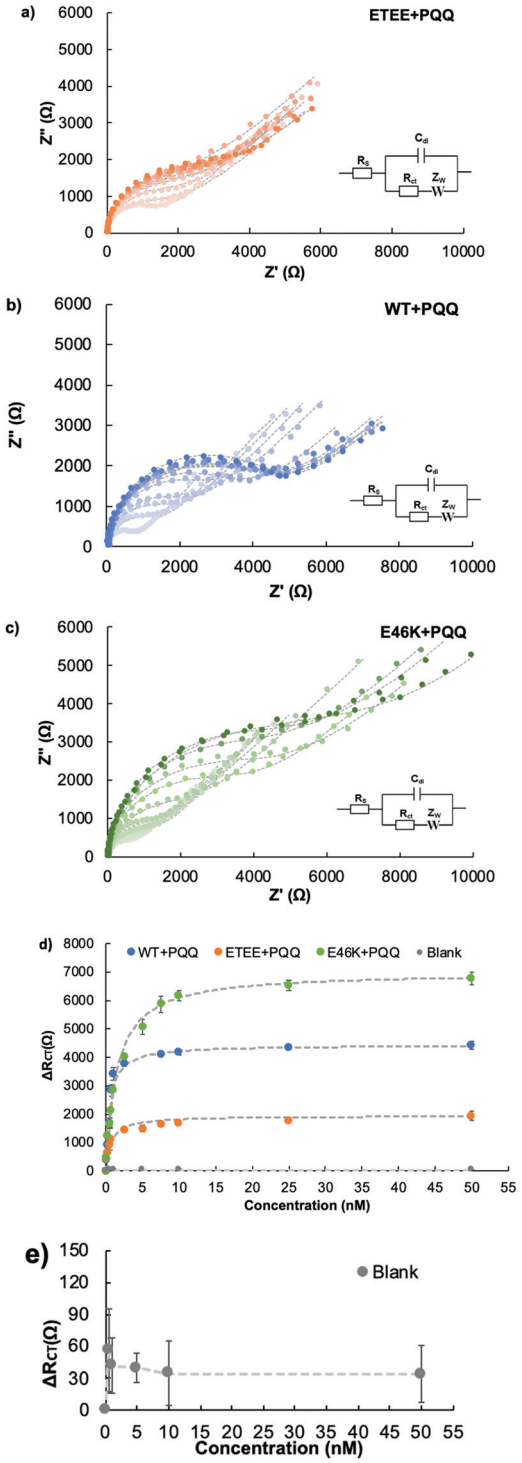

Fig. 7 Nyquist plots of α-syn peptides in the presence of increasing concentrations of PQQ (0.1 nM to 50 μM) at the SPEs modified with (a) ETEE, (b) WT, and (c) E46K. EIS data were fitted against a modified Randles equivalent circuit (as shown in the insets). ΔR_{CT} was calculated as the R_{CT} of peptide-modified SPEs after interaction with PQQ minus the R_{CT} of peptide-modified SPEs minus the R_{CT} of bare SPEs as shown in eqn (1). (d) Plot for the dependence of ΔR_{CT} on the concentration of PQQ at peptide-modified SPEs and (e) plot for the dependence of ΔR_{CT} on the concentration of PQQ at bare SPEs. Data were fitted against a modified Randles equivalent circuit to extrapolate the R_{CT} values and plotted against the concentration of PQQ. Error bars represent the standard deviation of triplicate measurements (n = 3).

reported the possible interaction of PQQ with the lysine residues of α-syn. In a follow-up study, Kim *et al.*[36] studied how the binding of PQQ with amyloid-β_{1-42} and mouse prion protein inhibited the fibrillation of these amyloid proteins. Zhu *et al.*[37] also described the binding of baicalein, another well-described antioxidant molecule, using lysine residues of α-syn that inhibited the formation of fibrils. Similarly, WT also contained the lysine side-chain as a possible binding site. However, since there was one less lysine to participate in the overall stabilization process, a higher K_D was observed. Lastly, for the ETEE, as a result of the complete lack of lysine residues, no electrostatic interaction took place resulting in the interaction of PQQ with the peptide *via* weak hydrogen bonding, hence loosely bound PQQ could be washed away with PBS resulting in a higher K_D value. Therefore, these results supported our hypothesis that lysine residues played a key role both as an initial contact site with PQQ and as a stabilizing factor of the PQQ–peptide complexes. The limit of detection of PQQ at a WT-peptide modified electrode was determined to be 100 nM based on the standard deviation of the ΔR_{CT} response of the blank PBS measurements and the slope of the calibration curve shown in Fig. 7d. The EIS measurements performed with PQQ at bare SPEs revealed that PQQ had negligible non-specific adsorption on the surfaces which did not significantly impact our studies (Fig. 7e).

Effect of PQQ on α-syn misfolding

Using a computational model, Rose *et al.*[38] have reported that Cu(II) increased the rate of α-syn misfolding by facilitating a long-range intramolecular contact between site-1 with residues 41–47 and site-2 with residues 56–62. In addition, both sites were among the seven groups that are lysine-containing mutant repeats. Therefore, it was critical to evaluate if PQQ prevented or suppressed the contact between these two sites on α-syn. As shown in Fig. 8, the SPEs were first modified with the 3-MPA-conjugated WT peptides containing site-1 residues 41–47 (WT-41–47). One group of WT-modified SPEs (n = 3) were then subjected to incubation with the peptides containing the site-2 residues 56–62 that were not conjugated with 3-MPA (WT-56–62). The second group of WT-modified SPEs (n = 3) was subjected to 1 mM of PQQ and allowed to be incubated overnight, and then the WT-56–62 was introduced after the WT + PQQ-modified SPEs were thoroughly rinsed. Both groups were evaluated by EIS and subsequently fitted with a modified Randles equivalent circuit to obtain the R_{CT} values. The bare SPEs were also incubated with thiol-free peptides alone to investigate whether the thiol-free peptides developed any non-specific adsorption issues. As shown in the Nyquist plots in Fig. 7, the thiol-free peptides displayed no significant non-specific adsorption on the bare SPE surfaces. A schematic illustration of the experimental design for protein–protein interactions can be found in Fig. S8.† As shown in Fig. 7, in the group of WT-modified SPEs where PQQ was not previously introduced, the R_{CT} increased two-fold after incubation with WT-56–62 peptides indicating the strong interaction between two peptide layers. In the group of WT + PQQ-modified SPEs

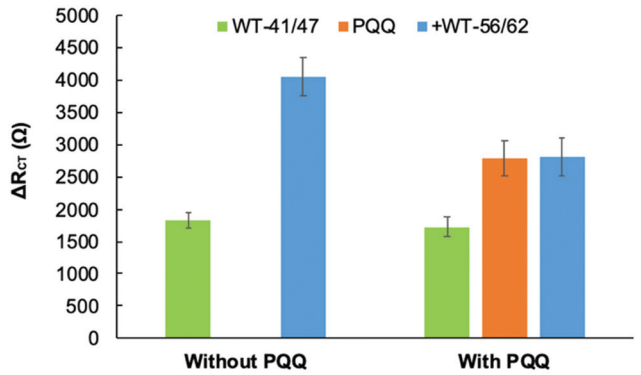

Fig. 8 Bar graph for the comparison of R_{CT} results of SPEs immobilized with 1 mM of thiolated-WT peptides with residues 41–47 (green), WT-modified SPEs incubated with 1 mM PQQ (orange), and WT-modified SPEs incubated with 1 mM non-thiolated peptides with residues 56–62 (blue). The ΔR_{CT} was calculated as the R_{CT} of peptide-modified SPEs before interaction with PQQ minus the R_{CT} of bare SPEs (without PQQ) and the R_{CT} of peptide-modified SPEs after interaction with PQQ minus the R_{CT} of bare SPEs (with PQQ). Error bars express the standard deviation of three independent measurements of each condition described in the figure (n = 3).

that were exposed to PQQ, the R_{CT} increased, as well, indicating the strong binding of PQQ to the surface-immobilized peptides. However, when WT-56–62 peptides were subsequently introduced, the R_{CT} showed no significant change. Therefore, we suggested that the presence of PQQ prevented the interaction between WT-41–47 and WT-56–62 peptides. Tsukakoshi *et al.*[39] reported that an esterified compound of PQQ, PQQ-trimethylester (PQQ-TME), had twice the blood–brain barrier permeability than PQQ *in vitro*. PQQ-TME also exhibited a higher inhibitory activity against the fibrillation of α-syn, prion protein and amyloid-β_{1-42} related to Alzheimer's disease. Recently, Ji *et al.*[40] have reported that agonist PQQ and suppressant (LY294002) changed cell cycle and apoptosis by regulating the PI_3K-AKT-$GSK_3\beta$ pathway in SH-SY5Y cells. Further studies on the synthesis of various esterified compounds of PQQ for the electrochemical detection of intramolecular interactions between PQQ-esters and α-syn peptides with residues 41–47 and 56–62 are under investigation in our laboratory.

Conclusions

The proof-of-concept study demonstrated the design and construction of a cost-effective and rapid electrochemical flow injection analysis assembly for the study of protein–small molecule interactions. Using the electrochemical setup and other spectroscopic techniques, we demonstrated that lysine was an important key amino acid residue to facilitate the interaction between PQQ and α-syn. HPLC, LC-MS and NMR results demonstrated the possible formation of the carbinolamine intermediates supporting the hypothesis that the α-syn–PQQ interaction was achieved *via* a Schiff base formation. Furthermore, it was demonstrated that the flow injection device allowed an efficient approach to determine the binding affinity between peptides and PQQ. Finally, PQQ was shown to suppress the binding between the residues 41–47 and 56–62 during the intramolecular rearrangement of α-syn that would provide useful information for the design of novel drug molecules targeting the early-stage aggregation of α-syn. These promising results demonstrated that the reported electrochemical system could enhance and streamline the rapid and cost-effective pre-screening of potential therapeutic molecules that interact with α-syn related to PD.

Author contributions

Shaopei Li: conceptualization; investigation; methodology validation; writing – original draft; writing – review & editing; Meissam Noroozifar: conceptualization; investigation; methodology validation; writing – original draft; writing – review & editing; Jiayun Zhou: conceptualization; investigation; methodology validation; writing – original draft; Kagan Kerman: conceptualization; methodology; data curation; funding acquisition; project administration; supervision; writing-review & editing.

Conflicts of interest

The authors declare no conflicts of interest.

Acknowledgements

K.K. acknowledges financial support from the Canada Research Chair Tier-2 award for "*Bioelectrochemistry of Proteins*" (Project no. 950-231116), the Ontario Ministry of Economic Development and Innovation (Project no. 35272), the Discovery Grant (Project no. 3655) from the Natural Sciences and Engineering Research Council of Canada (NSERC), and the Canada Foundation for Innovation (Project no. 35272). Special thanks are due to Tony Adamo at the TRACES center of UTSC for his tremendous support in HPLC and LC/MS analyses. We also acknowledge D. C. Burns and K. Z. Demmans for their guidance in the NMR spectroscopy studies at the CSICOMP NMR facility at the Department of Chemistry, University of Toronto.

References

1 L. Stefanis, *Cold Spring Harb. Perspect Med.*, 2012, **4**, a009399.
2 G. Fusco, A. De Simone, T. Gopinath, V. Vostrikov, M. Vendruscolo, C. M. Dobson and G. Veglia, *Nat. Commun.*, 2014, **5**, 3827.
3 D. Eliezer, E. Kutluay, R. Bussell and G. Browne, *J. Mol. Biol.*, 2001, **307**, 1061–1073.

4 C. C. Jao, B. G. Hegde, J. Chen, I. S. Haworth and R. Langen, *Proc. Natl. Acad. Sci. U. S. A.*, 2008, **105**, 19666–19671.
5 W. Zhang, T. Wang, Z. Pei, D. S. Miller, X. Wu, M. L. Block, B. Wilson, W. Zhang, Y. Zhou, J. S. Hong and J. Zhang, *FASEB J.*, 2005, **19**, 533–542.
6 K. C. Luk, V. Kehm, J. Carroll, B. Zhang, P. O'Brien, J. Q. Trojanowski and V. M.-Y. Lee, *Science*, 2012, **338**, 949–953.
7 E. Junn and M. M. Mouradian, *Neurosci. Lett.*, 2002, **320**, 146–150.
8 P. Ranjan and A. Kumar, *ACS Chem. Neurosci.*, 2017, **8**, 2235–2246.
9 E. Deas, N. Cremades, P. R. Angelova, M. H. R. Ludtmann, Z. Yao, S. Chen, M. H. Horrocks, B. Banushi, D. Little, M. J. Devine, P. Gissen, D. Klenerman, C. M. Dobson, N. W. Wood, S. Gandhi and A. Y. Abramov, *Antioxid. Redox Signal.*, 2016, **24**, 376–391.
10 J. H. Lu, M. T. Ardah, S. S. K. Durairajan, L. F. Liu, L. X. Xie, W. F. D. Fong, M. Y. Hasan, J. D. Huang, O. M. A. El-Agnaf and M. Li, *ChemBioChem*, 2011, **12**, 615–624.
11 J. Bieschke, J. Russ, R. P. Friedrich, D. E. Ehrnhoefer, H. Wobst, K. Neugebauer and E. E. Wanker, *Proc. Natl. Acad. Sci. U. S. A.*, 2010, **107**, 7710–7715.
12 K. Kimura, M. Takada, T. Ishii, K. Tsuji-Naito and M. Akagawa, *Free Radicals Biol. Med.*, 2012, **53**, 1239–1251.
13 Y. Itoh, K. Hine, H. Miura, T. Uetake, M. Nakano, N. Takemura and K. Sakatani, in *Advances in Experimental Medicine and Biology*, Springer, New York, NY, 2016, vol. 876, pp. 319–325.
14 J. Kim, R. Harada, M. Kobayashi, N. Kobayashi and K. Sode, *Mol. Neurodegener.*, 2010, **5**, 20.
15 K. Sode, S. Ochiai, N. Kobayashi and E. Usuzaka, *Int. J. Biol. Sci.*, 2007, **3**, 1–7.
16 M. Zhu, S. Rajamani, J. Kaylor, S. Han, F. Zhou and A. L. Fink, *J. Biol. Chem.*, 2004, **279**, 26846–26857.
17 A. Binolfi, L. Quintanar, C. W. Bertoncini, C. Griesinger and C. O. Fernández, *Coord. Chem. Rev.*, 2012, **256**, 2188–2201.
18 J. J. Zarranz, J. Alegre, J. C. Gómez-Esteban, E. Lezcano, R. Ros, I. Ampuero, L. Vidal, J. Hoenicka, O. Rodriguez, B. Atarés, V. Llorens, E. G. Tortosa, T. Del Ser, D. G. Muñoz and J. G. De Yebenes, *Ann. Neurol.*, 2004, **55**, 164–173.
19 C. L. Baird and D. G. Myszka, *J. Mol. Recognit.*, 2001, **14**, 261–268.
20 I. G. Siller, J. A. Preuss, K. Urmann, M. R. Hoffmann, T. Scheper and J. Bahnemann, *Sensors*, 2020, **20**, 1–16.
21 J. Maldonado, M. C. Estévez, A. Fernández-Gavela, J. J. González-López, A. B. González-Guerrero and L. M. Lechuga, *Analyst*, 2020, **145**, 497–506.
22 Q. Sun, J. Wang, M. Tang, L. Huang, Z. Zhang, C. Liu, X. Lu, K. W. Hunter and G. Chen, *Anal. Chem.*, 2017, **89**, 5024–5029.
23 M. F. Bergamini, A. L. Santos, N. R. Stradiotto and M. V. B. Zanoni, *J. Pharm. Biomed. Anal.*, 2005, **39**, 54–59.
24 E. Paleček, V. Ostatna, M. Masařík, C. W. Bertoncini and T. M. Jovin, *Analyst*, 2008, **133**, 76–84.
25 M. Masařík, A. Stobiecka, R. Kizek, F. Jelen, Z. Pechan, W. Hoyer, T. M. Jovin, V. Subramaniam and E. Paleček, *Electroanalysis*, 2004, **16**, 1172–1181.
26 P. Lopes, H. Dyrnesli, N. Lorenzen, D. Otzen and E. E. Ferapontova, *Analyst*, 2014, **139**, 749–756.
27 I. Álvarez-Martos and E. E. Ferapontova, *Anal. Chem.*, 2016, **88**, 3608–3616.
28 Q. Zhang, S. Chen, S. Yu, J. Qin, J. Zhang, Q. Cheng, K. Ke and F. Ding, *Neuropharmacology*, 2016, **108**, 238–251.
29 T. Inoue and J. R. Kirchhoff, *Anal. Chem.*, 2000, **72**, 5755–5760.
30 M. Kobayashi, J. Kim, N. Kobayashi, S. Han, C. Nakamura, K. Ikebukuro and K. Sode, *Biochem. Biophys. Res. Commun.*, 2006, **349**, 1139–1144.
31 N. Kobayashi, J. Kim, K. Ikebukuro and K. Sode, *Open Biotechnol. J.*, 2009, **3**, 40–45.
32 M. A. Shah, P. R. Bergethon, A. M. Boak, P. M. Gallop and H. M. Kagan, *Biochim. Biophys. Acta*, 1992, **1159**, 311–318.
33 I. Szymańska, H. Radecka, J. Radecki and R. Kaliszan, *Biosens. Bioelectron.*, 2007, **22**, 1955–1960.
34 I. Grabowska, H. Radecka, A. Burza, J. Radecki, M. Kaliszan and R. Kaliszan, *Curr. Alzheimer Res.*, 2010, **7**, 165–172.
35 K. Bandyopadhyay, L. Shu, H. Liu and L. Echegoyen, *Langmuir*, 2000, **16**, 2706–2714.
36 J. Kim, M. Kobayashi, M. Fukuda, D. Ogasawara, N. Kobayashi, S. Han, C. Nakamura, M. Inada, C. Miyaura, K. Ikebukuro and K. Sode, *Prion*, 2010, **4**, 26–31.
37 M. Zhu, S. Rajamani, J. Kaylor, S. Han, F. Zhou and A. L. Fink, *J. Biol. Chem.*, 2004, **279**, 26846–26857.
38 F. Rose, M. Hodak and J. Bernholc, *Sci. Rep.*, 2011, **1**, 11.
39 K. Tsukakoshi, W. Yoshida, M. Kobayashi, N. Kobayashi, J. Kim, T. Kaku, T. Iguchi, K. Nagasawa, R. Asano, K. Ikebukuro and K. Sode, *ACS Chem. Neurosci.*, 2018, **9**, 2898–2903.
40 H. Ji, J. Ma, L. Chen, T. Chen, S. Zhang, J. Jia, X. Yang, C. Guo, Z. Xiao and P. Niu, *Neurotox. Res.*, 2020, **38**, 266–273.